Dynamic shading of a building envelope based on rotating polarized film system controlled by one-dimensional cellular automata in regular tessellations (triangular, square and hexagonal)

Machi Zawidzki

Department of Architecture, Massachusetts Institute of Technology
77 Massachusetts Ave. 7-304G, Cambridge, MA 02139, U.S.A.
T: +1 617 253 0781, F: +1 627 253 9407, E: zawidzki@mit.edu

The original prototype of the cellular automaton (CA) shading system (CASS) for building facades was based on rectangular array of cells and used liquid crystal technology. This paper introduces polarized film shading system (PFSS) – an alternative approach based on opto-mechanical modules whose opacity is a function of the rotation of polarized film elements. PFSS in regular tessellations: triangular, square and hexagonal are discussed. Simulations for each type of tessellation are presented and visualized. Visual attractiveness of emergent CA patterns manifested by “particles” and “solitons” is discussed.

Keywords: adaptive architecture; organic architecture; building envelope; CA shading.

1. Introduction: towards intelligent building envelope

In architecture, building envelope (BE) besides the size and shape of a building, is the most apparent statement of designer's creativity. Too often, however, architectural decisions are based on aesthetics only, which has the evident disadvantage of limiting the potential of performance improvement [1]. BE as the interface between the exterior and interior serves several important functions, such as:

- protection from external factors, as it improves security and reduces the levels of noise and pollution,
- protection from climatic changes (temperature, humidity, glare),
- provision of natural light and visual contact with the environment, or the visual isolation from the exterior if required.

Furthermore, today's BEs often play a significant role in energy conservation by reducing the demands for artificial lighting, by either collecting solar energy or shielding from its excess. Rising energy prices and the need for reduction of the greenhouse gas emissions necessitate the development of intelligent buildings (IB) that operate on an energy-efficient and user friendly basis [2]. IB is to provide a productive and a cost-effective environment through optimization of its four basic elements: structure, systems, services & management and the interrelationships between them [3]. The biggest challenge is to optimize the trade-off between energy consumption and occupants’ comfort [2]. The climatic requirements for the interior conditions vary among the occupants, however in relatively narrow ranges. Conversely, the exterior conditions vary substantially both in circadian and annual cycles. Therefore, BE of IB should also be somewhat intelligent, that is adapt both to the occupants' requirements and to the variable outdoor conditions.

1.1 Daylighting: Visual and thermal comfort indoors and energy conservation

“No space, architecturally, is a space unless it has natural light.” - Louis Kahn

The main benefits of daylighting as a design strategy:

– Economy / ecology: D. substantially reduces the energy consumption and greenhouse gasses emissions [4,5];

- Physiology: D. is an effective stimulant to the human visual and circadian systems;
- Well-being: D. provides high illuminance and permits excellent color discrimination and color rendering; enables occupants to see both a task and the space well, and to experience some environmental stimulation [6], working by daylight is believed to result in less stress and discomfort.
- Society: those of higher status in organizations are often given spaces closer to/with more windows [6].

For the survey of literature on the benefits of daylight through windows see [7].
A study of the shading effects presented in [8] showed that in hot and humid climates such as Hong Kong, daylighting is always an energy saver. In the Nordic climates, the direct solar gains can greatly reduce the heating demand during cold seasons, however, it can also cause glare [5]. It is also worth noting that: glare is much more tolerated from a daylight source than from its artificial equivalent [9], significantly less incidents of eyestrain are reported by people whose workstations received large proportions of natural light [10], and high luminance contrasts were more tolerated when the window occupied a large portion of the visual field [11].
The nature of thermal and visual comfort differ substantially. Post occupancy evaluations showed that occupant satisfaction with the room temperature correlates strongly with the possibility of the occupants to change their working environment (e.g. operable windows or temperature control of heating or cooling system) and their sensation that the environment actually changed (e.g. perceived temperature increases or decreases) [12]. On the other hand, occupants' satisfaction correlates poorly with the actual room temperature and the temperature sensation [13]. In the case of daylight control, when manually operated shading devices are available, people tend to set them and then rarely to change them. However, photocontrolled shading devices also need overriding occupant controls if they are to be accepted [14].
This conforms with the classic observation in modern psychology, that perceived control can moderate stress reactions [15]. For example, when people were given the opportunity to end an aversive noise (although they did not use it), they did not experience the negative aftereffects on task performance that were observed in people who had not had that opportunity [16].
Moreover, personal preference of illuminance levels and the degree of the glare discomfort vary, and desired quantities of additional electric light depend on the type of task and the distance from a window. For a survey of literature on how different factors influence human comfort indoors see [17].
Daylight offers a dynamic, changing pattern to stimulate the eye. It also provides a very wide range of illuminance: from 0 to over 25 000 lx. It is much beyond commonly required values which range from 10 to 1000 lx, that is from the lowest level of color discrimination to the bright appearance [18].
There are a number of systems for controlling these variances to appropriate levels. Light coming through windows can be controlled by (e.g. anidolic) blinds, louvers, sun directing glass, laser-cut and prismatic panels, light (guiding) shelves to name the most common systems. Daylight can be also harvested, usually from a roof, and redistributed inside a building with so called light pipes. For a survey of such systems see [19]. However, no universal solution exists. A daylight control system should be selected according to climatic characteristics, that is the predominant sky type and the latitude at the building site. [20] recommends that its careful integration with the rest of a building’s design should begin early in the design process to produce a high-quality environment. Daylight control and modeling is particularly difficult in urban areas since the illuminance on the external face of the window is not only a function of the light coming directly from the sun and sky, but also of the component reflected from the ground, and obstructions above the horizon [21].

1.2 The outside view
Traditionally, in many cultures, a window is not only the source of natural light, but as research indicates, there is a psychological need for visual contact with exterior. Views that incorporate

horizon and sky are the most satisfactory, particularly after dark. In fact, night scenery of cities and their skylines seem to be equally, or even more appealing to human eye than natural scenes [22]. Importance of visual landscapes is not limited to aesthetics, but also includes a range of influences on emotional states, in other words the individuals' psychological well-being. Therefore it should be given explicit attention in planning and design decisions [23]. Positive effect of natural scenery on restorative process of surgical patients have been demonstrated in [24], and therapeutic advantages of urban scenery over natural views for chronically understimulated patients have been suggested in [25].
It seems that constructing an entirely artificial device which would satisfy all the requirements mentioned above is not economically feasible. Therefore the most realistic approach for intelligent building envelope (IBE) is to control the incoming light through natural apertures of buildings – windows.

1.3 Smart windows
Windows with dynamic optical properties seem a straightforward solution for IBE. The technology of electrochromism, liquid crystal switching and electrophoretic switching was discovered and made publicly in the 1970s and the 1980s, respectively. However, according to [26] the progress has been slow. After several decades, dynamically tintable, or so-called smart windows (SW) became available to the market. The required properties for SW for building energy control applications: solar transmission and reflection, switching voltage, memory, cycling lifetime and operating temperature at bleached and colored states have been documented in [27]. The technologies of electrochromic, gasochromic, liquid crystal and electrophoretic or suspended-particle devices were examined and compared for dynamic daylight and solar energy control in buildings in [26]. Based on surveys among architects, professionals accredited by Leadership in Energy and Environmental Design and window manufacturers, the most desired properties regarding the performance of SW are:

1. integration with other coatings, e.g. low thermal emissivity (low-e),
2. glare reduction,
3. consistent-looking tint changes regardless of window size,
4. light control to any point between the dark and clear transparent state,
5. high blockage of UV light,
6. fast switching speeds.

In the list above the properties particularly relevant to IBE and CASS are underlined. It shows that they share much of technological fields. However, due to low cost effectiveness and durability, the applications of SW in architecture are still rather sparse. According to [28], there is, however, gradually growing interest in SW among the architects due to:

1. the large scale introduction of smart glass,
2. steadily rising demand for windows and doors,
3. consumer interest in quality-of-life enabling technologies,
4. positive impact of daylighting,
5. movement toward increased energy efficiency.

In the list above the issues particularly relevant to IBE and CASS are underlined. It also shows similarities in architects' motivations.

However, although many SW systems are promising, none of them is truly satisfactory. For detailed analysis see [26].
As shown above, the requirements for BE are not only difficult to meet, but often contradictory. Moreover, creating buildings that can alter their appearance is one of perpetual dreams in architecture.

1.4 An example of adaptive building envelope: the Arab World Institute
One of the most recognized examples of adaptive BE was realized in the Arab World Institute

(AWI) [29] in Paris, France, where an array of 24×10 metallic screen compounds were installed as shown in figure 1.1. The screen unfolds with moving geometric motifs to control incoming daylight and to articulate aesthetic quality of the Arab architecture, as shown in figure 1.

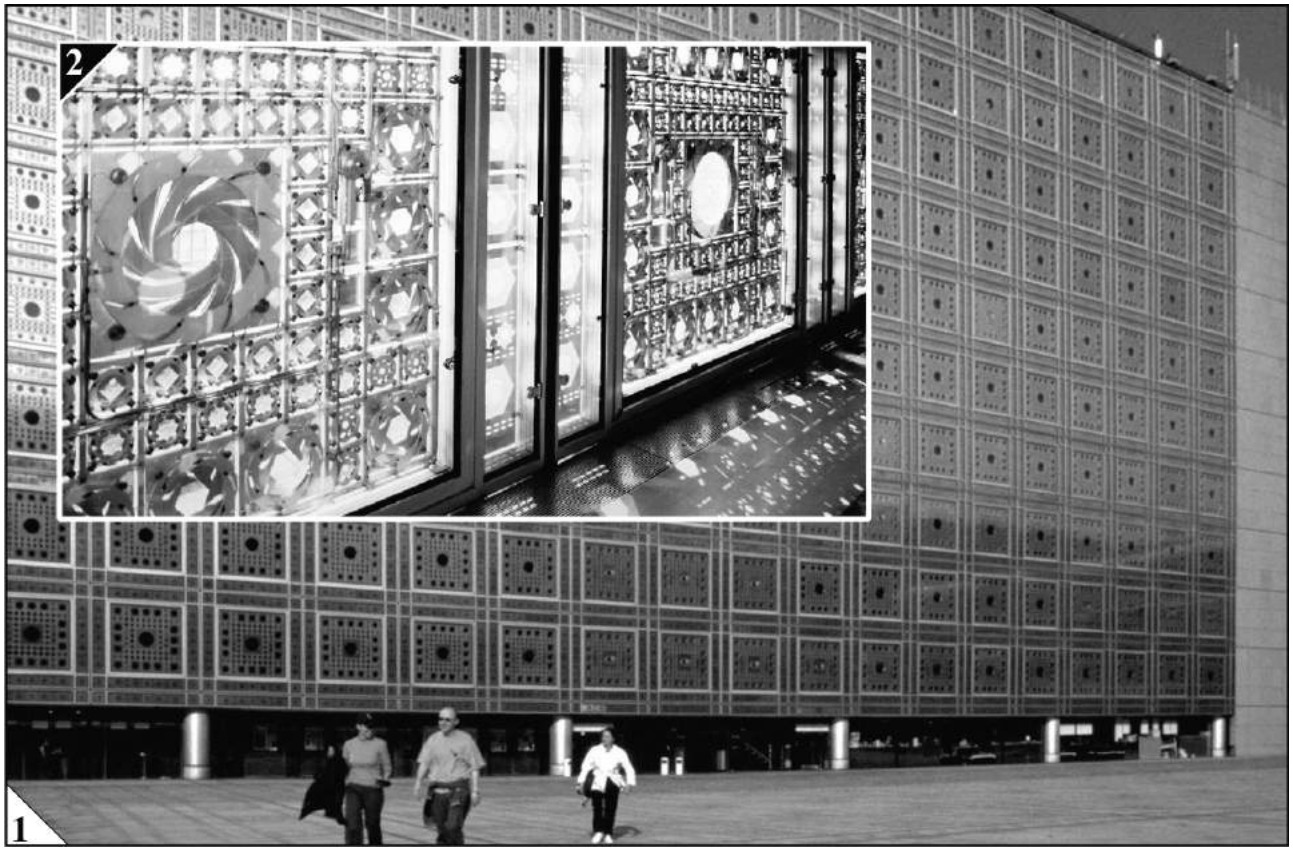

Figure 1: 1). A photograph of a part of the south facade of AWI. The shading system is comprised of 240 mechanical compounds. Some of them are in open position. 2). Diaphragms seen from the inside. Photographs © Transnational Lighting Detectives.

Compounds are controlled independently and each of them is comprised of several diaphragms. This highly sophisticated mechanical system is an impressive architectural feature, however, prone to failures which have already been reported soon after completion in 1987. Despite its limited transmission dynamics (approximately 1:4) [30], and the fact that it presently serves merely as a decoration, it remains as one of the most successful embodiment of the concept of IBE, where at least conceptually, the adaptivity and aesthetics are fully integrated.
An alternative idea based on cellular automaton (CA), so called CA-shading system, CASS for short, has been proposed in [31]. In CASS, the facade is divided into identical units which form a lattice for CA, and only the top row of cells is controlled directly. The pattern in the entire array is the result of the local interactions determined by the update rules, the same for each cell. The system is therefore homogenous like many biological systems [32], and emerging patterns exhibit certain “organic” integrity as shown in figure 2.

Figure 2: A visualization of CASS. The size of CA cells is approximately 1×1 m.

For interactive demonstrations illustrating mapping of CA on various surfaces see [33,34].

1.5 Cellular automata

Cellular automata (CA) are discrete complex systems which can be regarded as a fully distributed computational system with local processing only of very simple components [35]. The practical applications of CA are limited mostly to modeling and simulation, also to optimization. Relatively few physical devices driven by CA have been constructed. Despite underlying simplicity, CA are capable of *strong emergence* – that is producing a property which is irreducible to its individual constituents [36, 37]. This phenomenon exhibits through patterns which often possess new and intriguing aesthetics which can be used in the field of design. The cells of CA are interconnected and respond to state of surrounding cells and their own current state according to local transition rules (TR). For example: (0,1,1) → **0** means that in one step of CA evolution, if the main cell (central position in the bracket) has value 1 and the values in the neighboring left and right cells are 0 and 1, respectively – the value in the main cell turns 0. Since in this case there are three binary cells, there are $2^3 = 8$ such TRs for this particular type. CA rule number is a decimal notation of TR outputs. E.g. CA defined by the following TRs: (1,1,1)→**1**,(1,1,0)→**0**, (1,0,1)→**0**, (1,0,0)→**1**, (0,1,1)→**0**, (0,1,0)→**0**, (0,0,1)→**1**, (0,0,0)→**0** is named "rule 146" ← $146_{10} = 10010010_2$ ← (1,0,0,1,0,0,1,0). In a case of 3 states (2,1,0) the rule number is a decimal notation of the sequence of ternary TR outputs etc.

The number of states is finite and the time steps are discrete. From practical perspective – each cell is identical. Although the fabrication of a single cell may not be trivial, it can be mass-produced at relatively low cost [38]. CA is defined by the number of possible states, type and size of neighborhood (radius), dimensionality, border and initial conditions (IC). Even among the simplest non-trivial, that is two-color (2C) one-dimensional (1D) radius-one (r1), so called elementary cellular automata (ECA), there are some that are capable of emergence.

It is common to present 1D CA as to show the history of generation changes, where each row corresponds to a step in the history. Every row becomes an IC for the next row and so forth as

shown in figure 3.

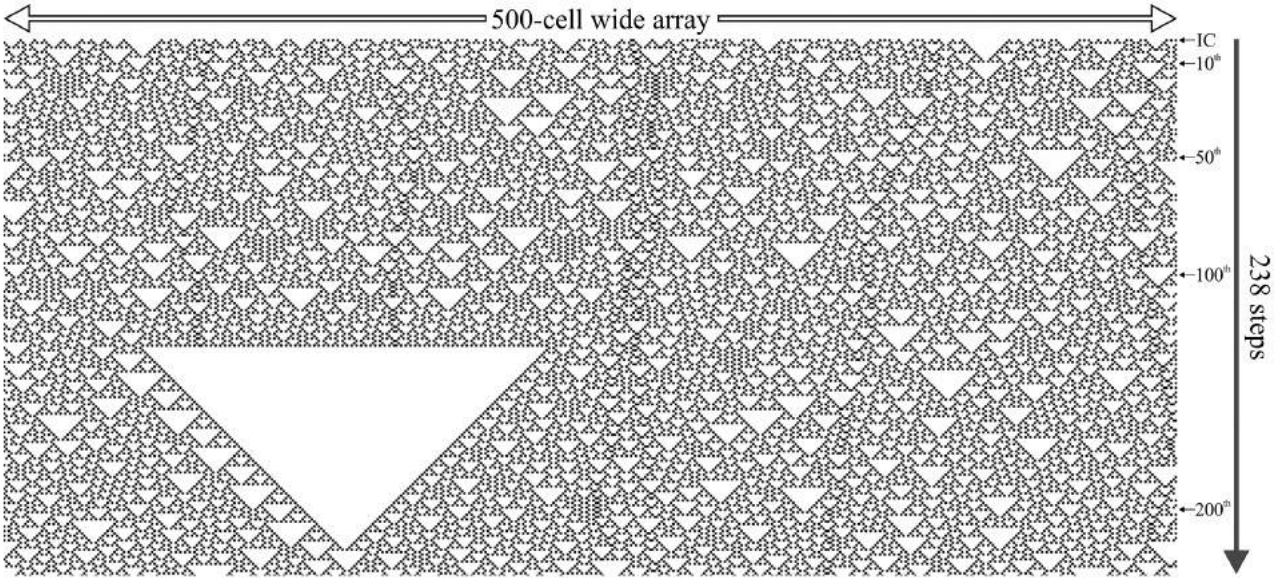

Figure 3: A surprising pattern formation – so called monolith, emerges after 130 steps of ECA rule 146 starting from certain IC.

In the case of general CA, at each step of evolution, explicit values from the main and all neighboring cells are taken for the computation of state of the main cell. The number of general 1D CA rules grows astronomically with the size of neighborhood and number of states. Therefore, when searching for the rules of desired behavior, it is often rational to explore different variations of automata before expanding the neighborhood or increasing the number of states. For example, at each step of evolution, totalistic (T) CA take the sum of all values (main + neighboring cells) and semi-totalistic (ST) CA take the explicit value in the main cell and sum of values in neighboring cells for the computation of state of the main cell [39]. So called half-distance rules can be created by shifting the successive rows, so the number of input cells becomes even. If an underlying cell is placed between the two cells above, it is called radius 1/2 (r-1/2) CA. For radii 3/2 (r-3/2) and 5/2 (r-5/2), the underlying cell is placed between the corresponding 4 and 6 cells, respectively. For a corresponding interactive demonstration see [40]. Higher-order CA depend not only on the present state of the cells, but also on their state in the past. For example in second-order CA (SOCA) the state of a cell at time $t+1$ depends not only on its neighborhood at time t, but also on its state at time $t-1$. Examples of these automata are shown in Table 1.

Table 1: Selected types of CA with examples

			Examples	
Type	Abbrev.	Cardinality	Local transition rules (TR)	Rule
General	-	256 (ECA)	(1,1,1)→**1**, (1,1,0)→**0**, (1,0,1)→**0**, (1,0,0)→**1**, (0,1,1)→**0**, (0,1,0)→**0**, (0,0,1)→**1**, (0,0,0)→**0**	146
Radius 2	r2	4.29×10^{9}	(1,1,1,1,1)→**1**, (1,1,1,1,0)→**1**, (1,1,1,0,1)→**1**, (1,1,1,0,0)→**0**, (1,1,0,1,1)→**0**, (1,1,0,1,0)→**0**, (1,1,0,0,1)→**1**, (1,1,0,0,0)→**1**, (1,0,1,1,1)→**1**, (1,0,1,1,0)→**0**, (1,0,1,0,1)→**0**, (1,0,1,0,0)→**1**, (1,0,0,1,1)→**1**, (1,0,0,1,0)→**1**, (1,0,0,0,1)→**1**, (1,0,0,0,0)→**0**, (0,1,1,1,1)→**1**, (0,1,1,1,0)→**0**, (0,1,1,0,1)→**0**, (0,1,1,0,0)→**0**, (0,1,0,1,1)→**0**, (0,1,0,1,0)→**1**, (0,1,0,0,1)→**1**, (0,1,0,0,0)→**0**, (0,0,1,1,1)→**0**, (0,0,1,1,0)→**0**, (0,0,1,0,1)→**1**, (0,0,1,0,0)→**1**, (0,0,0,1,1)→**1**, (0,0,0,1,0)→**0**, (0,0,0,0,1)→**0**, (0,0,0,0,0)→**0**	38188 17080
3-color	3C	7.62×10^{12}	(2,2,2)→**0**, (2,2,1)→**0**, (2,2,0)→**0**, (2,1,2)→**0**, (2,1,1)→**1**, (2,1,0)→**1**, (2,0,2)→**1**, (2,0,1)→**0**, (2,0,0)→**0**, (1,2,2)→**0**, (1,2,1)→**0**, (1,2,0)→**1**, (1,1,2)→**1**, (1,1,1)→**1**, (1,1,0)→**1**, (1,0,2)→**0**, (1,0,1)→**1**, (1,0,0)→**1**, (0,2,2)→**1**, (0,2,1)→**0**, (0,2,0)→**0**, (0,1,2)→**1**, (0,1,1)→**0**, (0,1,0)→**0**, (0,0,2)→**1**, (0,0,1)→**1**, (0,0,0)→**1**	237 834 554 3463
Totalistic	T	16	3 → **1**, 2 → **0**, 1 → **1**, 0 → **0**	10
Semi-totalistic	ST	64	(1, 3) →**0**, (1, 2) →**0**, (1, 1) →**0**, (1, 0) →**0**, (0, 3) →**1**, (0, 2) →**0**, (0, 1) →**0**, (0, 0) →**1**,	9
Half-distance	r-1/2	16	(1, 1) →**0**, (1, 0) →**0**, (0, 1) →**1**, (0, 0) →**1**	3
3-color half-distance	3C r-1/2	19683	(2,2)→**2**, (2,1)→**0**, (2,0)→**1**, (1,2)→**1**, (1,1)→**1**, (1,0)→**2**, (0,2)→**0**, (0,1)→**2**, (0,0)→**2**	14237
3-color half-distance totalistic	3Cr-1/2T	243	4 → **2**, 3 → **2**, 2 → **1**, 1 → **0**, 0 → **1**	226
Totalistic second-order	T SO	128	6 → **0**, 5 → **1**, 4 → **1**, 3 → **0**, 2 → **1**, 1 → **0**, 0 → **0**	52

All these variations of automata are considered for the proposed shading system and exemplified further in the text.

2. Cellular automaton-based shading in regular tessellations

Since the opacity of IBE must be controllable, the particular CA used for shading, besides exhibiting interesting aesthetics, must also have the following properties:

1. The control of average density of entire array to be set by IC only.
2. To render wide range of average densities, ideally from full transparency to opacity.

The search methodology and selection process of the automaton for the original CASS – 2C1DR2 CA code {3818817080,2,2}, CA_{SH} for short, is described in [31]. The first, second and third values in the CA_{SH} code correspond to decimal enumeration of TR outputs, the number of possible states and neighborhood size (radius), respectively.

2.1 Three regular tessellations

The prototype of CASS proposed in [38] is based on square grid, which is one of three, regular, also called “Platonic” tilings. The remaining two are: triangular and hexagonal. The symmetry group of regular tilings is transitive on the tiles, in other words, they are homogenous with respect to vertices, tiles and edges and are strongly edge-homogenous [41]. This is equivalent to an edge-to-

edge tiling by congruent regular polygons. This property has been widely used in architectural practice since antiquity, and the first systematic mathematical treatment was done in the early 17th century by Kepler in [42]. The properties of regular tessellations in the context of architectural design and particularly in daylight control (shading) are collected in table 2.

Table 2: Comparison of three regular tessellations in the context of CA shading.

	Architectural properties	Practicality for CASS
□	Rectangular or square meshes are prevalent in architecture and engineering. Most of the joints and connections in buildings are at the right angle. Regular square tiling are extremely rare in macro scale in nature (e.g. bismuth and galena crystals [43], cobwebs of *Cyrtophora citricola* [44]). It is, however, the most common type used in human constructions. Therefore, it is perhaps not particularly visually attractive. Nonetheless, it is perceived rather neutral since it tends not to overwhelm the impression of a displayed pattern.	The easiest to apply. Each CASS module is identical.
▽	Triangles are the only polygons that are rigid in plane [45]. This property is particularly useful in architecture and engineering. Regular triangular meshes do not occur naturally in macro scale and are also relatively rare in built environment (e.g. girders). Therefore this type seems relatively visually interesting. However, it has strong appearance, less neutral than square grid.	Some triangles point up, and some – down, therefore two types of modules may be necessary for CASS.
⬡	Since it is the only regular tessellation without single points of contact, the patterns appear as the most coherent. Although relatively rare in human design, it is more often encountered in macro scale in nature (e.g. honeycomb, basalt columns). Therefore it carries certain visual organic appeal.	There are two kinds of hexagonal tilings – "zigzag" (Z) and "armchair" (A) (see figure 9). Z requires one type of module, while A may require two for CASS.

Examples of naturally occurring regular tessellations in the macro scale are shown in figure 4.

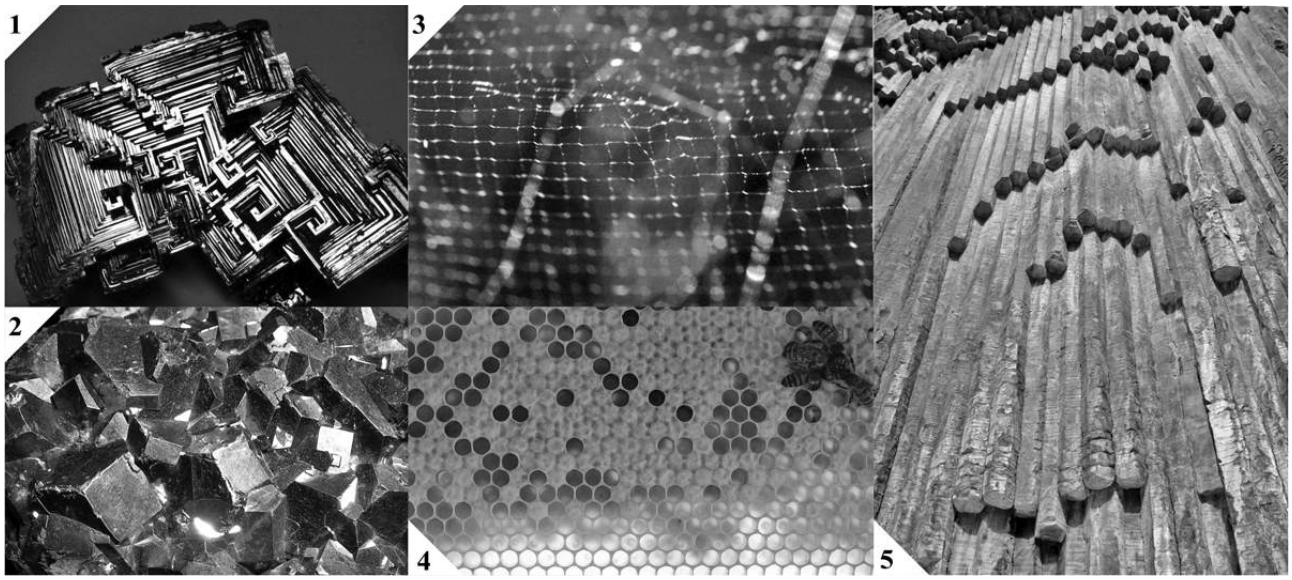

Figure 4: 1. Bismuth crystal, (photo©amazingrust.com); 2. Galena crystals (©irishminerals.com); 3. *Cyrtophora citricola* cobweb (©vi.wikipedia.org); 4. Honeycomb (©oldvan.com); 5. Basalt columns (©Colin Carlaw).

Various applications of CA in other tessellations than rectangular have already been documented. E.g. life-like rules on r1 Moore's neighborhood in triangular lattice have been studied in [46]; the computational universality of an 8-state triangular reversible partitioned CA has been demonstrated in [47]; and the effect of simple memory on a particular reversible, structurally dynamic CA in triangular tessellation has been demonstrated in [48]. For overview of CA, in particular the Game of Life (GL) in triangular, pentagonal and hexagonal tessellations see [49]; for the corresponding interactive demonstration see [50]. Modest size examples of GL in triangle, square, and hexagon planar topologies and hierarchical hexagonal grid on the sphere intended for modeling of biogeographical, ecological and epidemiological processes on the globe have been presented in [51]. Because hexagonal grid does not present spurious symmetries of the square lattice it has been implemented for wildfire spreading prediction in [52]. [53] explores GL on geodesic sphere, whose all facets are triangular. For an illustrative animation see [54], and for an interactive demonstration of ST CA on icosahedral geodesic sphere see [55].

2.2 The aesthetics of cellular automata and CASS

Visual attractiveness of CA can be attributed to their capability of emergence – the phenomenon which is characteristic to natural systems. According to [56], emergence is *a property of a complex system that is not exhibited by its individual component parts determined from a model of the system*. It is manifested in CA by the simultaneous occurrence of boundaries between the domains, which take form of boundaries or “particles”, that is small regions of cells separating two domains and persisting for a relatively many time steps. They may be stationary or may move; they may themselves exhibit a pattern that is temporally invariant, periodic, or even disordered [57]. Particular type of particle emerges in the so-called “solitons” - moving persistent structures which pass through one another while preserving their identities [58]. In this paper simple inspection of the spatio-temporal patterns and/or statistical regularities in the CA cell values was sufficient for the validation of the emergence. However, [59] proposed two complementary methods to automatically filter the changing configurations of spatial dynamical systems and extract coherent structures in CA: *local sensitivity*, which calculates the degree to which local perturbations alter the system, and picks out autonomous features; and *local statistical complexity*, which calculates the amount of historical information required for optimal prediction and identifies the most highly organized features.

The judgment of visual attractiveness of BE is more difficult than the aesthetics of pure CA pattern. Even the same CA pattern in different tessellations has different visual impact (see figure 12). BE is an integral part of architectural design, which according to [60] has over 2000 definitions. Nevertheless, CASS introduces new aesthetic possibilities, as illustrated with a number of examples further in text. Two as full visualizations (figures: 2 & 25) and the rest as patterns in various grids (figures: 12 – 19).

3. Rotating-polarized-film shading system

Although the prototype of CASS [38] was based on liquid crystal (LC) technology, the original concept was imagined as an opto-mechanical system of square plates made of polarized glass [31]. It was, however, easier to build the prototype with LC elements, which was not not the most economical choice. Although technology constantly evolves and prices tend to decrease, LCs are still relatively expensive both in terms of fabrication and running cost. They require approximately 5 W/m^2 of continuous power in the activated state [61]. In the prototype, the size of shading elements was approximately 12×12 mm. Moreover, according to [26] the transmittance modulation has been found poor for commercial LC windows. In addition, the LC windows have been found instable for UV radiation and as a result inappropriate for long-term exterior building applications.

This paper further explores the original approach called here polarized film shading system (PFSS), where shading elements are composed of two polygonal sheets of normally-white polarized films.

The size of PFSS module will be approximately ten times larger than the module of the original prototype. The fabrication cost of the entire system is expected to be substantially lower. One of the PFSS parts is fixed, and the other rotates. Opacity of PFSS units is proportional to the angle of rotation: at parallel position, that is 0°, the opacity is minimal and at crossed position, that is 90°, it is maximal. In idealized PFSS, opacity is direct function of rotation and reaches full range of values from 0 and 1. The minimal and maximal opacity occurs at $k\times180°$ and $k\times180°+90°$, respectively; where $k\in\mathbb{N}$.
Since states of CA are discrete, it is also natural to limit the rotation angles of polygonal elements to discrete, so called dihedral rotations (DR). The number of DRs for triangle, square, and hexagon is 3, 4 and 6, respectively.
It is assumed that for clarity of patterns displayed on BE, as well as for the shading practicality, the difference in opacity levels should be maximal. The number and range of extreme opacity achievable by PFSS depend on the initial angle (IA) of rotation and the number of DRs. For example, square PFSS (DR = 4) will at most produce only two distinct opacity levels as shown in figure 5.

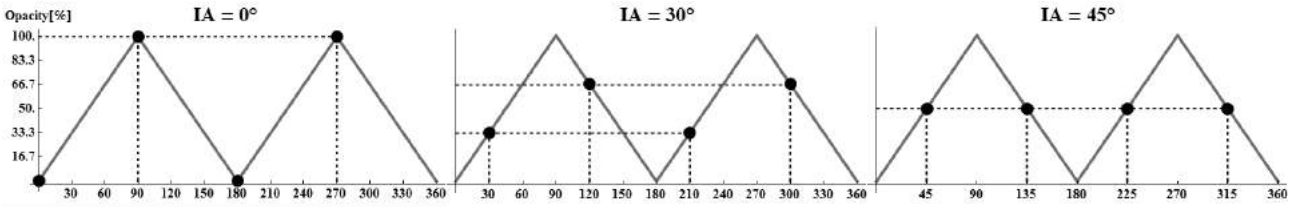

Figure 5: The opacity levels rendered by square PFSS at three different IAs. Black dots indicate opacity levels at four consecutive DRs.

In the first case shown in figure 5, IA = 0° and the extreme opacity levels are 0 and 1. At IA of 30°, the range of opacity is narrower, that is from 33.3 to 66.7%. IA equal to 45° will give the same 50% opacity regardless of the rotation angle.
Opacity rendered by PFSS depend on the polygon type and IA. To illustrate the possible opacity ranges for different PFSS setups, the IAs have been sampled at 1° for triangle, square and hexagon. Next, for each IA the opacities at each DR relevant to the polygon type have been calculated. The statistical dispersions of those sets have been measured by the median absolute deviation (MAD), which is a common and robust measure of the variability of a univariate sample of quantitative data. Figure 6 shows the plots of MADs of the opacities for triangular, square and hexagonal PFSS.

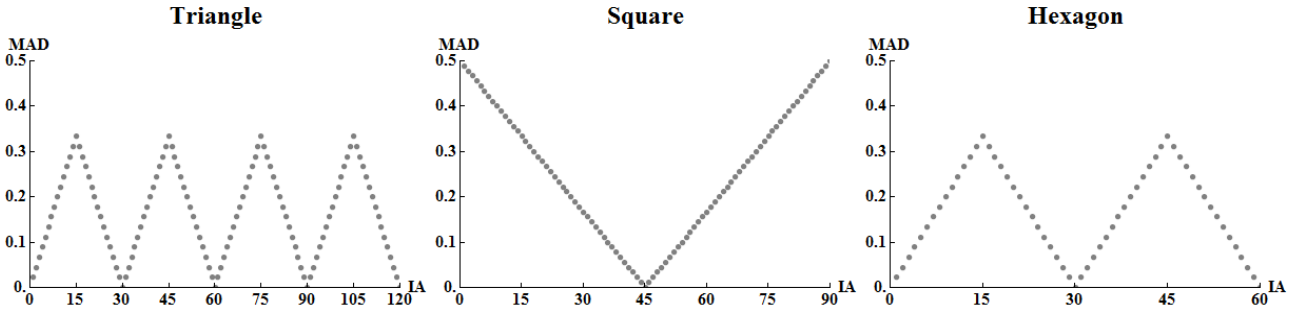

Figure 6: MADs of opacity levels for PFSS on regular tessellations.

As figure 6 indicates, IA that results in the maximal MADs are: for triangular PFSS: 15°, 45°, 75° and 105°, for square PFSS: 0° and 90°, and for hexagonal: 15° and 45°. The sequence of opacity rendered for given DRs also depends on IA. For example in the case of triangular PFSS, at IA of 15°, three consecutive opacities are: 16.7% (minimal), 50% (medium), and 83.3% (maximal). The corresponding MAD[{0.167, 0.5, 0.833}] = 0.333 (see Fig. 6). The sequence for IA of 45°: medium, minimal, maximal, as shown in figure 7.

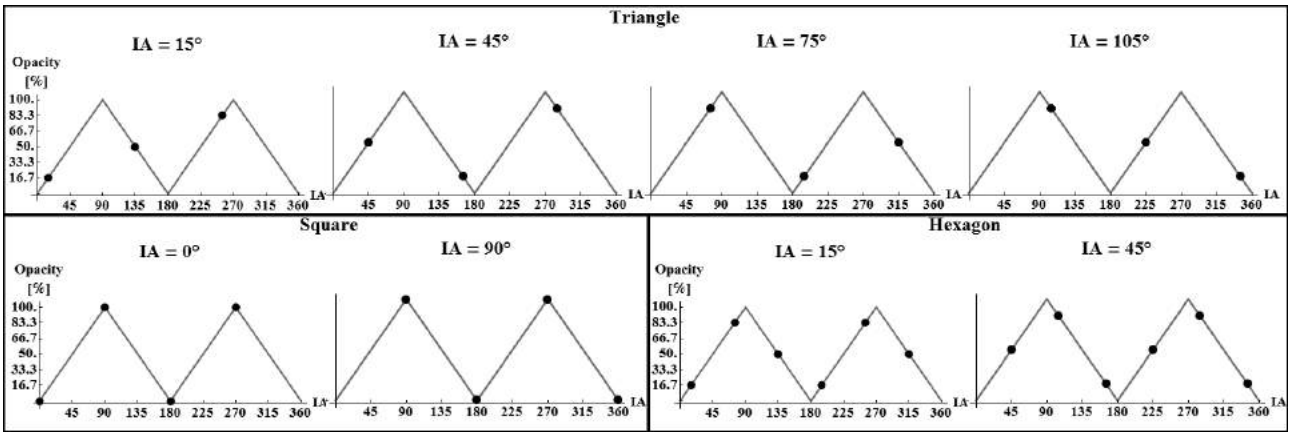

Figure 7: The sequences of opacities of maximal diversity.

Figure 8 illustrates opacity changes that correspond to the leftmost plot for each PFSS type shown in figure 7.

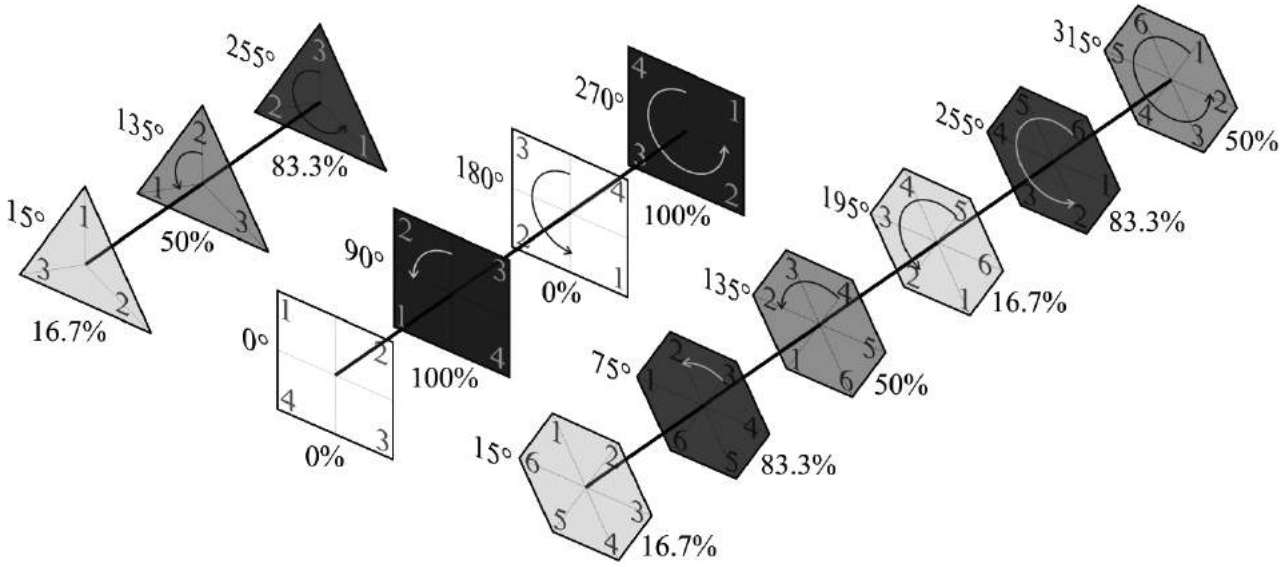

Figure 8: Opacity as a function of dihedral rotation for idealized PFSS on regular tessellations.

As figures 7 and 8 indicate, PFSS in triangular, square, and hexagonal tessellations have at maximum 3, 2 and 3 distinct opacities, respectively. However, only the square PFSS renders extreme values from 0 to 100%. The triangular and hexagonal ones render three shades of gray: 16.7%, 50% and 83.3%. These shading parameters are collected in table 3. IAs were selected so opacity grows monotonically with rotation angle.

Table 3. Distinct opacities of PFSS in regular tessellations

States	Tessellation:	Triangular			Hexagonal			Square	
2	IA [°]	30			30			0	
	Angle [°]	30	150	270	30	90	150	0	90
	Opacity [%]	33.3	33.3	100	33.3	1	33.3	0	100
3	IA [°]	15			165				
	Angle [°]	15	135	255	165	225	285		
	Opacity [%]	16.7	50	83.3	16.7	50	83.3		

As table 3 indicates, it is also possible to set up IAs for triangular and hexagonal tessellations, so the number of distinct states will be reduced. For IA = k×30°, where $k \in \mathbb{N}$, the number of states

becomes 2, with the extreme values of either 33.3 and 100% or 0 and 66.7%. Therefore it is also possible to implement 2C CA with them. These are the values for idealized system, in actual physical device the ranges of opacity values will be narrower.
PFSS operates similarly to the common convention of presenting history of evolution of 1D CA. A row of cells receives input from a row above and becomes IC for a row below, and so forth. This process continues in cascade and propagates down the entire array of cells (see figure 3). For an interactive demonstration illustrating this process see [62]. The idea of physical realization of PFSS is based on modules which are comprised of both input and output units. The output unit becomes one of the inputs for modules in the row below as shown in figure 9.

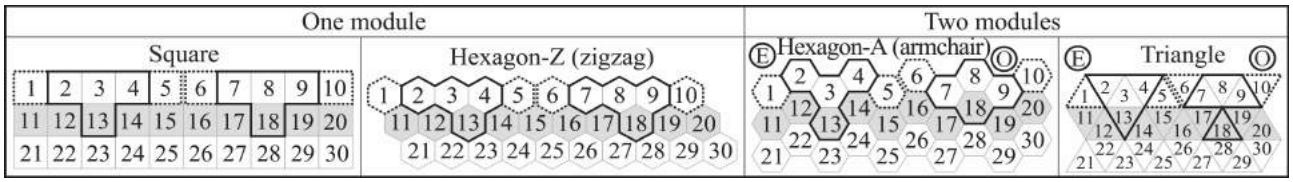

Figure 9: PFSS modules for 1D r1 and r2 CA in regular tessellations. Neighborhoods of sample modules are outlined in black. The r2 neighborhood is indicated by dotted lines.

As figure 9 indicates there are two possible arrangements of cells in hexagonal tessellation. So called “zigzag” tessellation (hexagon-Z) requires one type of module, and “armchair” tessellation (hexagon-A) requires two modules of different shapes: O and E.
Once value in an input cell has been set, it does not change or reset unless IC in the row above changes, as shown in figure 10.

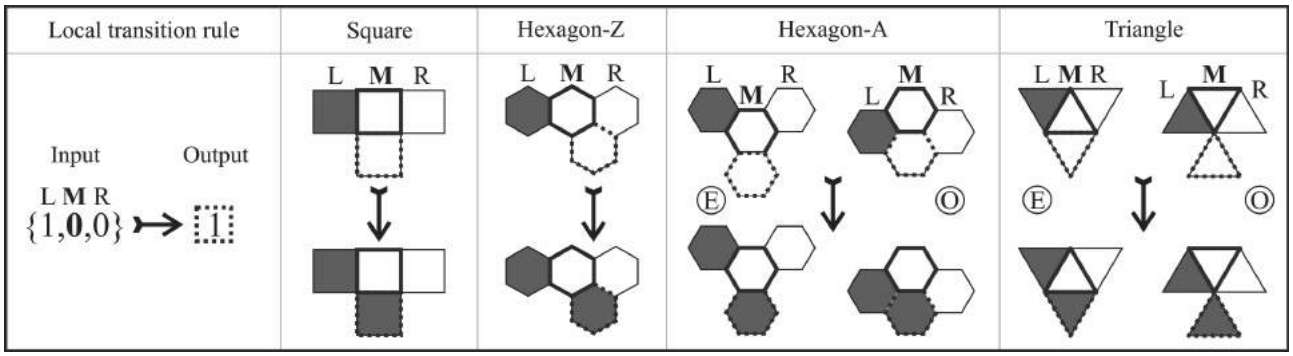

Figure 10: TR {1,0,0} → 1, and realization by square, hexagonal and triangular PFSS modules. M, L and R stand for main, left and right cells, respectively.

Figure 11 shows pattern of ECA rule 110 realized by PFSS modules from figure 9, starting from the same IC.

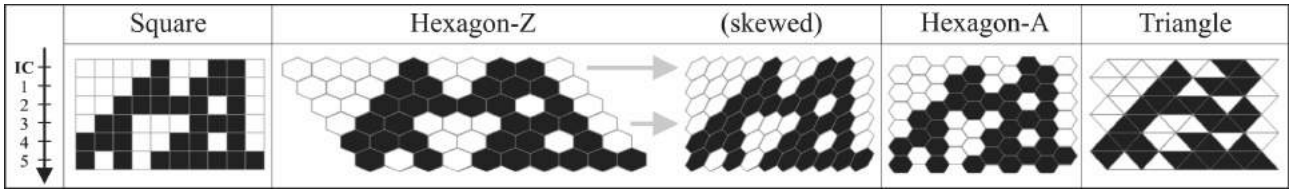

Figure 11: 5 steps of ECA evolution from IC: {0,0,0,0,1,0,0,1,1,0}. Hexagon-Z is also shown skewed to match the other grids. For comparison, grids have been scaled along vertical axis so the rows of cells are aligned horizontally.

For an illustrative demonstration of CA in regular grids see [63]. The original CA_{SH} can be implemented by four types of PFSS as shown in figure 12.

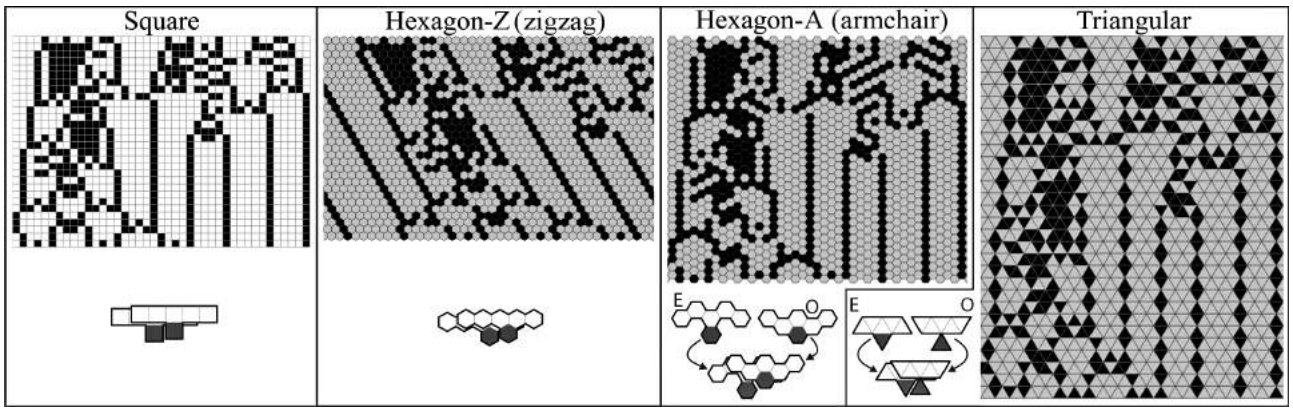

Figure 12: CA_{SH} (rule {3818817080,2,2}) realized by PFSS in regular tessellations. The shades of gray on arrays reproduce opacity values achievable by a particular PFSS. Two modules for each tessellation are shown schematically.

Square PFSS can realize any 2C1D CA, the hexagonal and triangular PFSS can realize both two (2C) and three (3C) state 1D CA.

3.1 Simulation

A number of simulations for each type of PFSS were performed in order to find the simplest, but visually interesting CA that can be applied on building facades. Since each type of PFSS: square, hexagonal and triangular have certain individual characteristics, the results are presented in three sub-sections.

3.1.1 SIMULATION IN SQUARE GRID: $PFSS_{SQ}$

As shown in table 3, PFSS based on square tessellation ($PFSS_{SQ}$) can realize only two-state CA. However, since each module is simple and identical, constructing it is relatively straightforward. As discussed in [31], the applicability of ECA for shading is very limited and consequently, r2 CA were explored. In this paper, however, instead of expanding the neighborhood of general CA, totalistic one-dimensional radius-one CA are considered. Furthermore, since there are only 16 such CA and none of them produce interesting patterns, finally second-order CA was proposed (1D2Cr1 T SO CA). In such a case there are two three-cell rows for input. The top and successive rows correspond to step $t-1$ and t of SOCA, respectively. Values in each cell can be either 0 or 1. Since there are six input cells in total, the number of such CA is $2^{6+1} = 128$. Although there are so few of them, many exhibit visually interesting behavior. Note: in principle PFSS is to be controlled by the very top row of cells, in the case of SOCA, however, the control may require two top rows of cells. A selection of particularly visually appealing such CA is shown in figure 13.

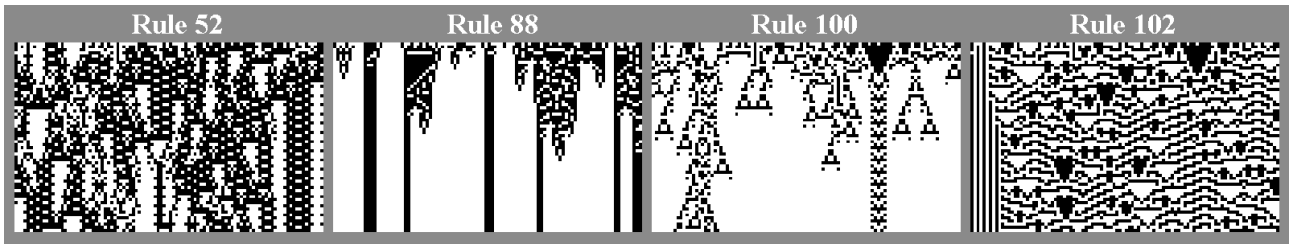

Figure 13: Example of four 1D2Cr1 T SO CA starting from the same coupled ICs.

3.1.2 SIMULATION OF PFSS IN HEXAGONAL GRID

PFSS in hexagonal tessellation can emulate both 2 and 3 state CA. The following examples are based on the latter. Depending on orientation, there are two types of hexagonal grids: “zigzag” – hexagon-Z, and “armchair” – hexagon-A, as shown in figures 9-12. Simulations are presented in two corresponding subsections.

3.1.2.1 Hexagon-Z: $PFSS_{HZ}$

As an example for PFSS based on “zigzag” hexagonal grid ($PSFF_{HZ}$), a one-dimensional three-color general half-distance radius 1/2 cellular automaton (1D3Cr-1/2 CA) is proposed. Since there are two input cells with three possible values (0,1,2), the number of such CA is $3^{3\times3}$ = 19,683. Some examples are shown in figure 14.

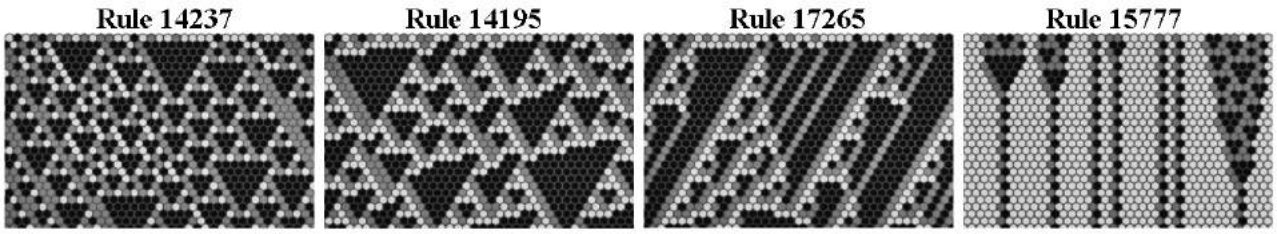

Figure 14: A few visually interesting 1D3Cr-1/2 CA.

It is also straightforward to implement regular, that is r1 3C CA. There are over seven trillions such rules, many producing intriguing patterns. Some examples are shown in figure 15.

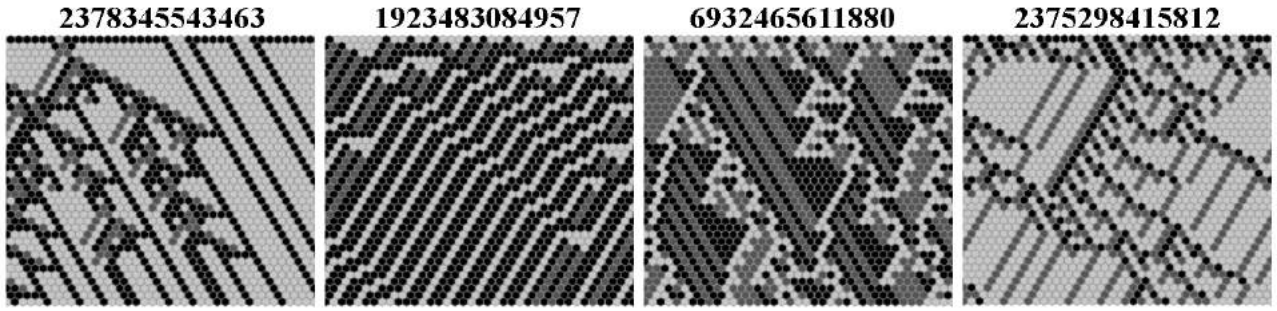

Figure 15: Four 1D3Cr1 general CA in hexagon-Z tessellation.

3.1.2.2 Hexagon-A: $PFSS_{HA}$

Alternatively, hexagons of a grid can be arranged in so called “armchair” (hexagon -A), and the corresponding shading system – $PFSS_{HA}$. As mentioned above, in such a case, emulating 1D CA requires two types of modules: E and O as shown in figures 9 and 10.

However, it is also possible to construct an array of cells using only one type of modules: E or O. Such systems derived from one-dimensional cellular automata, are called two-dimensional cellular automata with specified offsets, and denoted here as 2D*CA. 2D*3Cr1CAs based on type O (hexagon-H_O) produce trivial patterns as shown in figure 16.

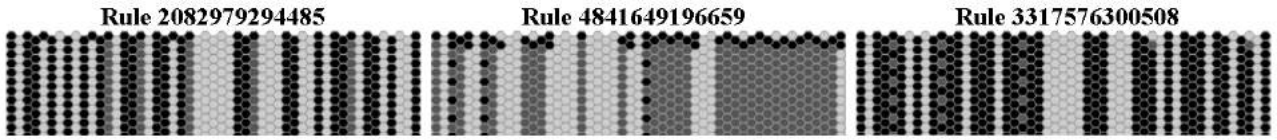

Figure 16: Some relatively visually appealing examples of 2D*3Cr1 hexagon-H_O CA.

3C systems based on hexagon-H_O tessellation demonstrate only class W1 and W2 behaviors, that is, nearly all initial patterns evolve quickly into a stable, homogeneous state or into oscillating structures. Type E (hexagon-H_E), however, is capable of all 4 kinds of behavior, including class W3, that is pseudo-random, and most importantly – W4 that is complex, as shown in figure 17.

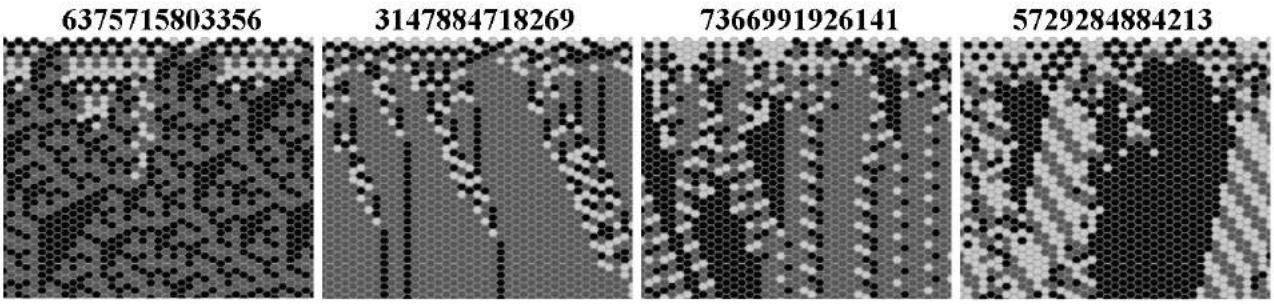

Figure 17: Some examples of 2D*3Cr1 hexagon-H_E CA.

3.1.3 SIMULATION IN TRIANGULAR GRID: $PFSS_T$

In the case of systems based on triangular tessellation ($PFSS_T$), emulating regular 1D CA also requires two types of modules, as shown in figures 9 and 10. However, in this case the implementation of half-distance CA seems particularly interesting for architecture. Such an arrangement leaves every other cell of the tessellation void, which can correspond to clear glass or solid walls. Such a $PFSS_T$ can be realized by three-color half-distance totalistic cellular automaton (1D3Cr-1/2 T CA). Although there are only 243 such automata, nearly half of them produce visually interesting patterns. Figure 18 shows them in square and dense grids (without voids) for legibility.

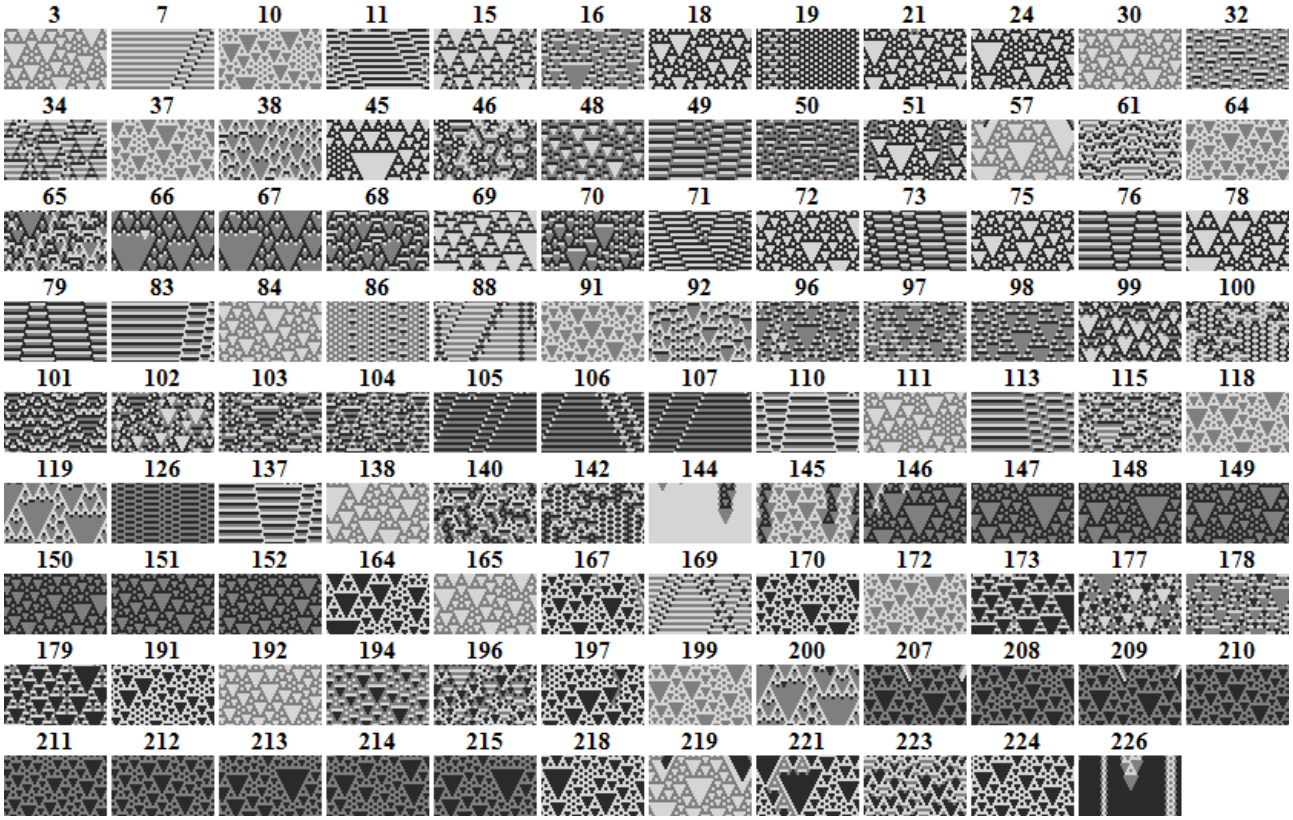

Figure 18: Selected 1D3Cr-1/2 T CA. Each rule starts from the same IC.

The most promising rules for architectural shading are: 106, 145, 207 and 226, as they meet the "shading criteria" to a certain extent. That is, they are relatively visually attractive and controllable to a certain degree by ICs. For more details on this selection method see [31]. Since the area of $PFSS_T$ is perforated in 50%, it should be taken in consideration, that pattern is not as legible as in other shading systems presented here. Nevertheless, some rules produce fairly legible patterns. The shortlisted rules from figure 18 are shown in figure 19 in the actual, perforated triangular grid.

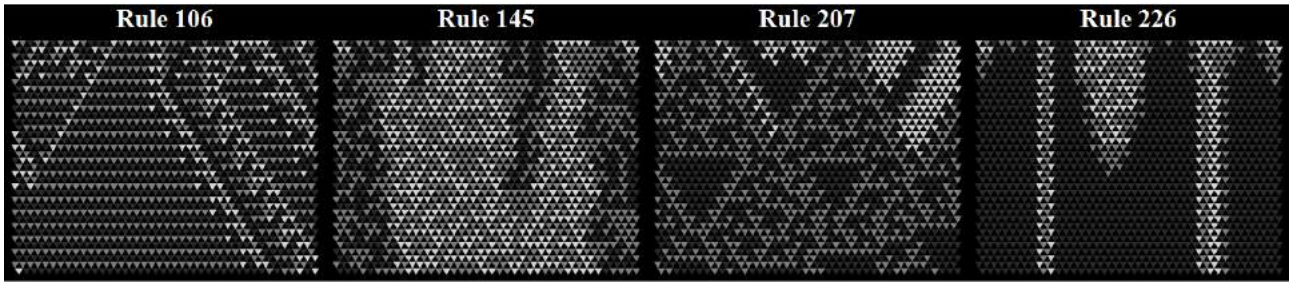

Figure 19. Selected $PFSS_T$ based on 1D3Cr-1/2 T CA starting from the same IC. The background is black, thus perforation also appears black.

4. The physical implementation

Alike the simulations physical implementation is also divided into sections that correspond to tessellation types.

4.1 Implementation of PFSS in square grid

The LC prototype presented in [38], $CASS_{LC}$ for short, is based on orthogonal tessellation and it has no moving parts. Although the concept of CASS is based on interactions among autonomous units, $CASS_{LC}$ is comprised of two components: CA control unit (CU) and the shading panel (SP). This decision was motivated by the following reasons:

1. to provide a hands-on experience of rather abstract concept of CA, therefore:
2. both CU composed of CA units and SP to be built by students,
3. system to be low-tech,
4. CA units to be programmable to emulate all 256 ECA.

CA units of CU are based on commonly available integrated circuits (CMOS), therefore they are much larger than intended for a real application, which most likely would combine field programmable gate arrays (FPGA) with printed circuit boards (PCB) [64]. On the other hand, due to high cost of LC elements, SP is much smaller than intended. Moreover, CU was built also to demonstrate “hardware automaton”. Each of its cell is equipped with a light emitting diode (LED) to display the CA action. This is also the reason why the CA circuits are not integrated with the shading elements, as it would be in the actual shading device. Figure 20 collects some of the $CASS_{LC}$ documentation.

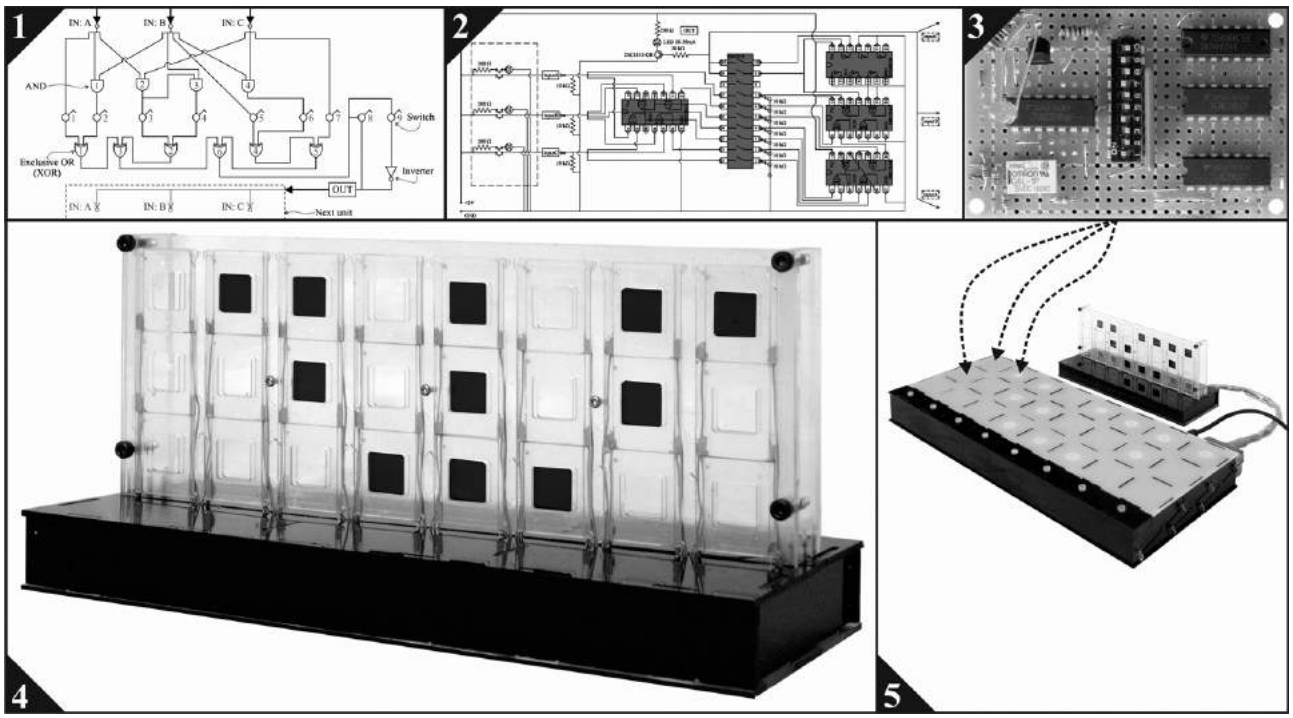

Figure 20: $CASS_{LC}$: 1. The scheme of the logic that emulates any of 256 ECA; 2. Electrical diagram of a CA unit 3. A photograph of a completed CA unit; 4. SP with some LC elements active (opaque); 5. SP displays the pattern produced by CU.

The mechanism of optical switching in LC is to change the orientation of LC molecules between two conductive electrodes by applying electric field. As mentioned above, they are not only expensive to make, but also to operate, since they require continuous power. Such LC system allows only two states for each cell. Some examples of much less expensive $PFSS_{SQ}$ units, which would be much larger and made of lightweight polarized film elements are shown in figure 21.

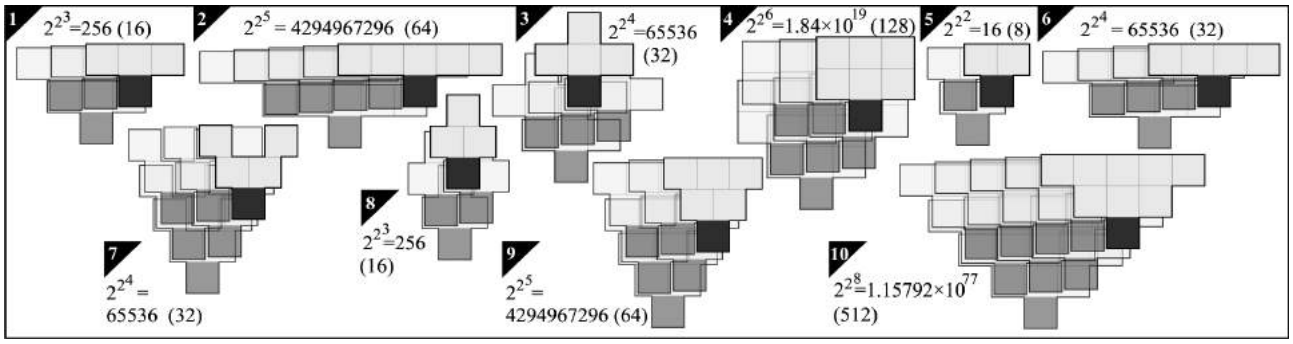

Figure 21: 2C CA realized by $PFSS_{SQ}$. 1–2): r1, r2, 3–4): SOCA, 5–6): r-1/2, r-3/2, 7–10): various 2D*CA. The numbers of all general rules are shown (totalistic rules – in parentheses).

Although this type of PFSS is the most straightforward to implement, it offers less possible states of cells than the other systems and its visual appearance seems to be not as pleasing.

4.2 Implementation of $PFSS_{HZ}$ and $PFSS_{HA}$

As mentioned above, major advantage of $PFSS_{HZ}$ is that it is visually appealing and there is only one type of module necessary to emulate any 1D CA. Some examples are shown in figure 22.

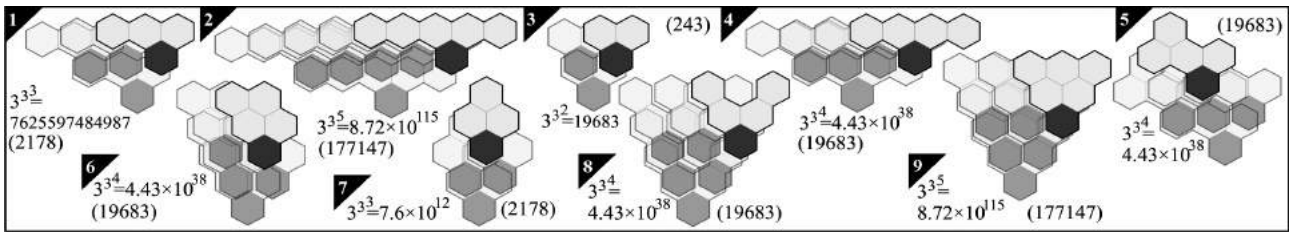

Figure 22: 3C CA realized by $PFSS_{HZ}$ 1–2): r1, r2, 3–4): r-1/2, r-3/2 , 5): r1 SOCA, 6–9): various 2D*CA.

Some examples of coupled modules for $PFSS_{HA}$ are shown in figure 23.

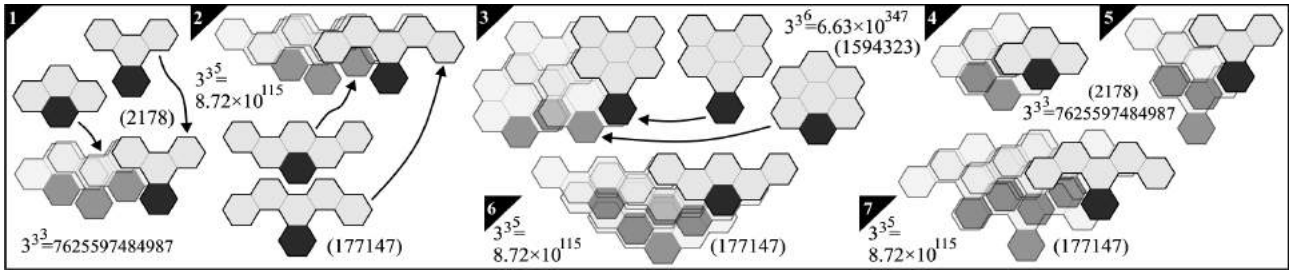

Figure 23: 3C CA realized by $PFSS_{HA}$ 1–2): r1, r2, 3–7): various 2D*CA.

4.3 Implementation of $PFSS_T$

Because triangular grid is not so rare in architecture (but not so common either), $PFSS_T$ can fit well to some particular design solutions. Some examples of units for dense and perforated $PFSS_T$ are shown in figure 24.

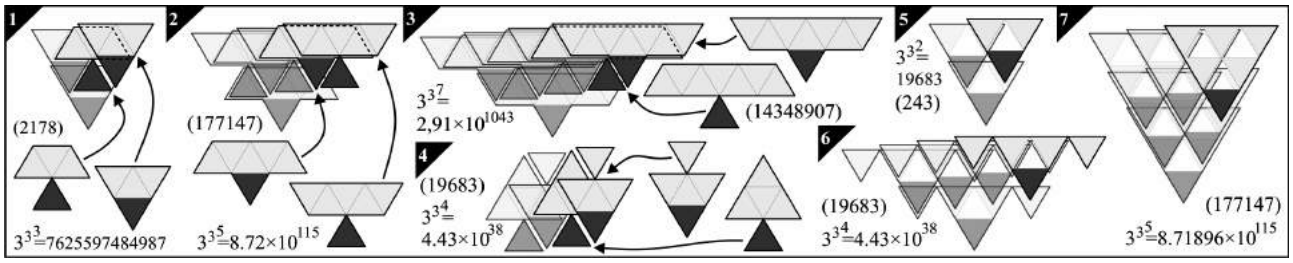

Figure 24: 3C CA realized by $PSFF_T$. 1–3): r1, r2, r3; 4): r1 SOCA; 5–6): r-1/2, r-3/2; 7): 2D*CA.

An example of implementation of 1D3Cr-1/2 T CA rule 226 with perforated $PFSS_T$ (specifically the module shown in figure 24.5) on a facade based on triangular prefabricated panels is visualized in figure 25.

Figure 25: A simulated example of a “living” cylindrical facade based on triangular panels. The left and central parts of pattern exhibit behaviors of class W2 and W4, respectively.

5. Critical discussion

A relatively recent survey of soft computing (SC) techniques in engineering design [65] points out that “existing approaches miss applicability or robustness (...)” and postulate expansion of existing methods to agent-based systems (ABS), among others. The project presented in this paper addresses both applicability and robustness.

The robustness analysis of CASS has been presented in [66]. Two types of permanent failures have been considered: a cell failure, when a single cell in ICs yields wrong (opposite) output, and a certain type of permanent (edge) failure [67], called there electric failure, when a single column of inactive cells splits the array in two independent sections. Although the patterns of shading automata are rather sensitive to these failures, their basic shading properties are relatively robust. Moreover, although the number of disturbed cells in the case of totalistic automaton (T CA 52) is the lowest, its basic shading properties, that is pattern density and distribution are disturbed the most. While the general automaton (CA_{SH}) is the most robust in respect to the pattern distribution, the semi-totalistic one (ST CA 666) is the most robust in respect to the pattern average density.

Moreover, the concept of modern ABS originates from widely discussed here cellular automata (CA), which can be considered as simplified ABS. According to [68]: “intelligent buildings can cope with social and technological change and are adaptable to short and long term human needs”. Presented here adaptive CA-based shading system contributes to the concept of intelligent built environment. However, as the introduction suggests, it is difficult to imagine an ideal solution for such complex problem as the ideal building envelope (BE). As pointed out in [69] “the notion of building adaptivity is a well known concept, however successful realizations are rather limited to high profile projects such as Santiago Calatrava's Milwaukee Art Museum or Peter Eisenman's Cardinal's stadium”. In the same paper an inexpensive fritted glass shading system (FGSS) is presented and retrofitting in a university building is documented. In FGSS each actuator is controlled individually, therefore there are no interactions among units that may trigger emergence. Moreover, the mechanical controls, although much simpler than in AWI (figure 1) might be problematic. The concept described here proposes an alternative approach. As in the building of AWI there is a design integrity between respective elements and the skin of a building as a whole. In the case of AWI it has more of a fractal nature with elements nested within each other. The idea

proposed here can be considered as more organic, where individual cells seem to have certain degree of freedom. In fact both systems are deterministic, however only the latter is capable of strong emergence.
Recent review of intelligent building construction [70] points out that although external static sunshades are most efficient among all types of sunshades, they satisfy shading needs only partially. Moreover, in [71,72] the authors notice that the common practice of focusing on a few engineering challenges or explicitly on sustainability in the early stage of design leads to buildings that might be sustainable considering their energy consumption but not in architectural aspects. In the approach proposed here, these aspects are integrated.
Although the physical device realizing the concept of CA-driven shading system is already operational, there is a number of conceptual, theoretical and practical issues to be solved. One of the main conceptual problems is how to balance controlling parts of PFSS corresponding to individual occupants or rooms with overall appearance of the building's envelope as a whole. Another closely related problem is to fine-tune the system to achieve sustainability and optimal energy consumption by incorporating the geographical location, season, external temperature, solar exposition, fenestration, etc. [73]. One of the possible solutions is to adjust IAs in given parts of PFSS. This would shift opacities of all affected modules. CASS also allows for non-uniform CA [74], that is automata whose individual cell TRs are not the same. Therefore is it also possible to subdivide PFSS into autonomous parts. In such a case, however, the aesthetic integrity of facade could be lost. Perhaps there is a solution in-between, where limited individual control is possible or where there are some interactions among zones of cells. For other possible practical issues related to CASS such as: the size of the cell, glare, etc. see [38]. A new prototype is presently being developed. The completion will answer many of these questions.

6. Conclusions

A project where creativity, practicality and economy meet was presented. Proposed shading system for buildings brings new, unparalleled aesthetics that emerges from collective behavior of homogenous, modular elements. For discussion on "man-made versus organic appearance" see [75]. A concept of rotating polarized film elements arranged in regular tessellation is simpler, low-maintenance, and is potentially more robust and affordable than existing systems for dynamic control of building envelopes.
The new method of improving indoor comfort connected with new aesthetics contributes also to the theory of design.
Presented here briefly creative process from nature-inspired cellular automata to a concept of feasible prototype for a robust shading system might inspire designers, architects and engineers for innovative work involving relatively new discoveries in computer science.

Acknowledgments

This is part of Singapore University of Technology & Design and Massachusetts Institute of Technology Postdoctoral Program (SUTD-MIT PDP). The research is titled: *Effective computational methods for grid and raster-based modeling of practical problems in architectural and urban design*.

References

[1] W. Wang, H. Rivard, R. Zmeureanu R, Floor shape optimization for green building design, Advanced Engineering Informatics 20 (4) (2006) 363–378.
[2] A. Ahmed et al, Mining building performance data for energy-efficient operation, Advanced Engineering Informatics 25 (2) (2011) 341–354.
[3] R. Caffrey, The intelligent building, an ASHRAE opportunity, ASHRAE Technical Data Bulletin 4 (1) (1985) 925–933.
[4] S. Aydinli, M. Seidl. 1986. Determination of the economic benefits of daylight in interiors concerned with the fulfillment of visual tasks, in M.S. Adepski, R. McCluney (Editors),

Proceedings I: 1986 International Daylighting Conference, 4-7 November 1986, Long Beach California USA, (1986) 145–151.
[5] M. Bodart, A. De Herde, Global energy savings in offices buildings by the use of daylighting, Energy and Buildings 34 (5) 2002 421–429.
[6] P. Boyce, Why Daylight ? Proceedings of Daylight ’98, International Conference on Daylighting Technologies for Energy Efficiency in Buildings, Ottawa, Ontario, Canada, (1998) 359–365.
[7] P. Boyce, C. Hunter, O. Howlett, The benefits of daylight through windows: Report, Lighting Research Centre, Rensselaer Polytechnic Institute, Troy, New York 2003.
[8] D.H.W Li, S.L. Wong, Daylighting and energy implications due to shading effects from nearby buildings, Applied Energy 84 (12) (2007) 1199–1209.
[9] W.K.E. Osterhaus, Discomfort glare from daylight in computer offices: how much do we really know? Proceedings of LUX Europa 2001, 9th European Lighting Conference, Reykjavik, Iceland, 18–20 June (2001) 448–456.
[10] I. Cowling, S. Coyne, G. Bradley, Light in Brisbane Office Buildings: A Survey, Research Report, Centre for Medical and Health Physics, Department of Physics, Queensland University of Technology, Brisbane, Australia, 1990.
[11] Y. Sutter, D. Dumortier, M. Fontoynont, The use of shading systems in VDU task offices: a pilot study Energy and Buildings 38 (7) (2006) 780–789.
[12] E. Gossauer, A. Wagner, User Satisfaction at Workspaces: A Study in 12 Office Buildings in Germany, CISBAT, Lausanne, Switzerland (2005).
[13] J.U. Pfafferott et al., Comparison of low-energy office buildings in summer using different thermal comfort criteria, Energy and Buildings 39 (2007) 750–757.
[14] A.D. Galasiu, J.A. Veitch, Occupant preferences and satisfaction with the luminous environment and control systems in daylit offices: a literature review, Energy and Buildings 38 (7) (2006) 728–742.
[15] J.A. Veitch, Psychological processes influencing lighting quality, Journal of the Illuminating Engineering Society 30 (1) (2001), pp. 124–140.
[16] D. C. Glass, J.E. Singer, Urban stress. New York: Academic Press, 1972.
[17] M. Frontczak, P. Wargocki, Literature survey on how different factors influence human comfort in indoor environments, Building and Environment 46 (4) (2011) 922–937.
[18] C. Cuttle, Lighting by Design, Elsevier, Amsterdam, 2003.
[19] J.T. Kim, G. Kim, Overview and new developments in optical daylighting systems for building a healthy indoor environment, Building and Environment 45 (2) (2010) 256–269.
[20] International Energy Agency. Daylight in buildings. a source book on daylighting systems and components, A Report of IEA SHC Task 21/ECBCS Annex 29, July 2000.
[21] P.R. Tregenza, Mean daylight illuminance in rooms facing sunlit streets, Building and Environment 30 (1) (1995) 83–89.
[22] J.L. Nasar, K. Terzano, The desirability of views of city skylines after dark, Journal of Environmental Psychology 30 (2) (2010) 215–225.
[23] R. S. Ulrich, Visual landscapes and psychological well-being, Landscape Research 4 (1979) 17–23.
[24] R.S. Ulrich, Affective and aesthetic responses to natural environment, in I. Altman, J. F. Wohlwill (Eds.), Behavior and the natural environment: Human behavior and environment, advances in theory and research, Vol. 6, New York: Plenum, 1983, pp. 85–125.
[25] R.S. Ulrich, View through a window may influence recovery from surgery, Science 27 April 1984, 224 (4647) (1984) 420–421.
[26] R. Baetens, B.P. Jelle, A. Gustavsen, Properties, requirements and possibilities of smart windows for dynamic daylight and solar energy control in buildings: A state-of-the-art review, Solar Energy Materials and Solar Cells 94 (2) (2010) 87–105.
[27] C.M. Lampert (Ed.), Failure and degradation modes in selected solar materials: a review (pp.19,30–46,75–77,A1–A8), prepared for The International Energy Agency, Solar Heating

and Cooling Program, Task10: Solar Materials R&D, May 1989.
[28] G. M. Sottile, 2004 Survey of United States architects on the subject of switchable glazings, Materials Science and Engineering B 119 (3) (2005) 240–245.
[29] The official website of the Arab World Institute: http://www.imarabe.org/index.html
[30] M. Fontoynont, Perceived performance of daylighting systems: lighting efficacy and agreeableness, Solar Energy 73 (2) (2002) 83–94.
[31] M. Zawidzki, Implementing Cellular Automata for Dynamically Shading a Building Facade, Complex-Systems 18 (3) (2009) 287–305.
[32] J. Kari, Theory of cellular automata: A survey, Theoretical Computer Science 334 (1–3), (2005) 3–33.
[33] M. Zawidzki, A Cellular Automaton Mapped on the Surface of a Cuboid, URL: http://demonstrations.wolfram.com/ACellularAutomatonMappedOnTheSurfaceOfACuboid/, an interactive demonstration (2010).
[34] M. Zawidzki, A Cellular Automaton Mapped on the Surface of a Cylinder, URL: http://demonstrations.wolfram.com/ACellularAutomatonMappedOnTheSurfaceOfACylinder/, an interactive demonstration (2012).
[35] D. Wolz, P.P.B. de Oliveira, Very Effective Evolutionary Techniques for Searching Cellular Automata Rule Spaces, Journal of Cellular Automata 3 (4) (2008) 289–312.
[36] R. Das, The Evolution of Emergent Computation in Cellular Automata, Ph.D. Thesis, Computer Science Department, Colorado State University, Ft. Collins USA, 1996.
[37] G. Faraco, P. Pantano, R. Servidio, The use of Cellular Automata in the learning of emergence, Computers and Education 47 (3) (2006) 280–297.
[38] M. Zawidzki, I. Fujieda, The prototyping of a shading device controlled by a cellular automaton, Complex-Systems 19 (2) (2010) 157–175.
[39] M. Garzon, Models of Massive Parallelism: Analysis of Cellular Automata and Neural Networks. European Association for Theoretical Computer Science, Springer Berlin Heidelberg. (1995).
[40] E. Pegg Jr, Half-Distance Rules with Low Resolution published at Wolfram Demonstrations Project: http://demonstrations.wolfram.com/HalfDistanceRulesWithLowResolution/
[41] D. Chavey, Tilings by regular polygons II: A catalog of tilings, Computers & Mathematics with Applications 17 (1–3) (1989) 147–165.
[42] J. Kepler, Harmonice Mundi, Lincii Austriae, 1619.
[43] Online periodic table reference website: http://periodictable.com/
[44] H. M. Peters, Functional organization of the spinning apparatus of Cyrtophora citricola with regard to the evolution of the web (Araneae, Araneidae), Zoomorphology 113 (3) (1993) 153 –163.
[45] G. Laman, On Graphs and Rigidity of Plane Skeletal Structures, J. Engineering Math. 4 (1970) 331–340.
[46] C. Bays, Cellular automata in the triangular tessellation. Complex-Systems 8 (1994) 127–150.
[47] K. Imai, A computation-universal two-dimensional 8 state triangular reversible cellular automaton. Theoretical Computer Science 231(2) (2000) 181–191.
[48] R. Alonso-Sanz, A structurally dynamic cellular automaton with memory in the triangular tessellation. Complex-Systems 17(1) (2007) 1–15.
[49] C. Bays, Cellular Automata and the Game of Life in the Hexagonal Grid, (2001). URL: http://www.cse.sc.edu/bays/h6h6h6/
[50] C. Bays, Cellular Automata in Triangular, Pentagonal and Hexagonal Tessellations. In: Meyers RA (ed.) Computational Complexity, Springer New York. (2012) 434–442.
[51] R.A. Kiester, K. Sahr, Planar and spherical hierarchical, multi-resolution cellular automata. Computers, Environment and Urban Systems 32 (2008) 204–213.
[52] G.A. Trunfio, Predicting Wildfire Spreading Through a Hexagonal Cellular Automata Model, in P.M.A. Sloot, B. Chopard, A.G. Hoekstra (Editors) Lecture Notes in Computer Science 3305 (2004) 385-394.

[53] J. Ventrella, Glider Dynamics on the Sphere: Exploring Cellular Automata on Geodesic Grids. Journal of Cellular Automata 6 (2–3) (2011) 245–256.
[54] J. Ventrella, Earth Day 2009 – A Spherical Cellular Automaton (2009). URL: http://www.ventrella.com/EarthDay/EarthDay.html
[55] M. Zawidzki, Semitotalistic Triangular Cellular Automata on a Geodesic Sphere, URL: http://demonstrations.wolfram.com/SemitotalisticTriangularCellularAutomataOnAGeodesicSphere, an interactive demonstration, (2014).
[56] A.K. Konopka, Systems Biology: Principles, Methods and Concepts Taylor and Francis. Taylor & Francis, Boca Raton, FL, (2006).
[57] J.E. Hanson, Encyclopedia of Complexity and Systems Science. In: Meyers RA (ed.) Cellular Automata, Emergent Phenomena, Springer, (2009) 768–778.
[58] K. Steiglitz, I. Kamal, A. Watson, Embedding computation in one dimensional automata by phase coding solitons. IEEE Transactions on Computers 37 (2) (1988) 138–145.
[59] C. Shalizi, R. Haslinger, J. Rouquier, K. Klinker, C. Moore, Automatic filters for the detection of coherent structure in spatiotemporal systems, Phys Rev E, (2006) 73:036104.
[60] M. Lesniakowska, Co to jest architektura. (In Polish) Warsaw: Agencja Kanon, 1996.
[61] C.M. Lampert, Large area smart glass and integrated photovoltaics, Solar Energy Materials and Solar Cells 76 (2003) 489–499.
[62] M. Zawidzki, Delayed CA, URL: http://demonstrations.wolfram.com/DelayedCA/, an interactive demonstration (2010).
[63] M. Zawidzki, One-Dimensional Cellular Automata on the Regular Tessellations, URL: http://demonstrations.wolfram.com/OneDimensionalCellularAutomataOnTheRegularTessellations/, an interactive demonstration (2012).
[64] S. M. Qasim, S. A. Abbasi, B. Almashary, An Overview of Advanced FPGA Architectures for Optimized Hardware Realization of Computation Intensive Algorithms, in Multimedia, Signal Processing and Communication Technologies (IMPACT 2009), Aligarh, India: IEEE, March 2009, 300–303.
[65] K.M. Saridakis, A.J. Dentsoras, Soft computing in engineering design – A review, Advanced Engineering Informatics 22 (2) (2008) 202–221.
[66] M. Zawidzki, K. Nishinari, Shading for building facade with two-color one-dimensional range-two cellular automata on a square grid, Journal of Cellular Automata, 8 (3-4) (2013) 147–163.
[67] C. Darabos, M. Giacobini, M. Tomassini, Performance and Robustness of Cellular Automata Computation on Irregular Networks, Advances in Complex Systems, 10 (1) (2007) 85–10.
[68] T. Derek, J. Clements-Croome, What do we mean by intelligent buildings? Automation in Construction 6 (5–6) (1997) 395–400.
[69] Z. Drozdowski, S. Gupta, Adaptive Fritting as Case Exploration for Adaptivity in Architecture, Proceedings of ACADIA09 the 29th Conference of the Association For Computer Aided Design In Architecture, Chicago, USA, 21-25 October (2009) 105–109.
[70] R.V. Ralegaonkar, R. Gupta, Review of intelligent building construction: A passive solar architecture approach, Renewable and Sustainable Energy Reviews 14 (8) (2010) 2238–2242.
[71] A. Schlueter, F. Thesseling, Building information model based energy/exergy performance assessment in early design stages, Automation in Construction 18 (2) (2009) 153–163.
[72] V. Granadeiro, J.P. Duarte, J.R. Correia, V.M.S. Leal, Building envelope shape design in early stages of the design process: Integrating architectural design systems and energy simulation, Automation in Construction 32 (2013) 196–209.
[73] LC Tagliabue, M. Buzzetti, B. Arosio, Energy Saving Through the Sun: Analysis of Visual Comfort and Energy Consumption in Office Space, Energy Procedia, 30 (2012) 693–703.
[74] M. Sipper, Co-evolving non-uniform cellular automata to perform computations, Physica D, 90 (1996) 193–208.
[75] M. Zawidzki, Application of Semitotalistic 2D Cellular Automata on a triangulated 3D surface. International Journal of Design & Nature and Ecodynamics 6 (1) (2011) 34–51.